Published in final edited form as:
Biochem J. 2012 November 15; 448(1): 83–91. doi:10.1042/BJ20120992.

Targeted oxidation of *Torpedo californica* acetylcholinesterase by singlet oxygen: Identification of *N*-formylkynurenine tryptophan derivatives within the active-site gorge of its complex with the photosensitizer methylene blue

Mathilde M. Triquigneaux[*,¶], **Marilyn Ehrenshaft**[*], **Esther Roth**[†], **Israel Silman**[†], **Yakov Ashani**[†], **Ronald P. Mason**[*], **Lev Weiner**[‡], and **Leesa J. Deterding**[§]

[*]Laboratory of Toxicology and Pharmacology, National Institute of Environmental Health Sciences, National Institutes of Health, DHHS, PO Box 12233 MD F0-03, Research Triangle Park, NC 27709

[†]Department of Neurobiology, Weizmann Institute of Science, Rehovoth, 76100 Israel

[‡]Department of Chemical Research Support, Weizmann Institute of Science, Rehovoth, 76100 Israel

[§]Laboratory of Structural Biology, National Institute of Environmental Health Sciences, National Institutes of Health, DHHS, PO Box 12233 MD F0-03, Research Triangle Park, NC 27709

Synopsis

The principal role of acetylcholinesterase (AChE) is termination of impulse transmission at cholinergic synapses by rapid hydrolysis of the neurotransmitter acetylcholine. The active site of AChE is near the bottom of a long and narrow gorge lined with aromatic residues. It contains a catalytic 'anionic' subsite (CAS) and a second peripheral 'anionic' site (PAS), the gorge mouth, both of which bind acetylcholine via π-cation interactions, primarily with two conserved tryptophans (Trps). It was earlier shown that generation of $^1O_2$ by illumination of methylene blue (MB) causes irreversible inactivation of *Torpedo californica* AChE (*Tc*AChE), and suggested that photo-oxidation of Trps might be responsible. In the present study, structural modification of the *Tc*AChE Trps induced by MB-sensitized oxidation was investigated using anti-*N*-formylkynurenine antibodies and mass spectrometry. From these analyses, we determined that *N*-formylkynurenine derivatives were specifically produced from Trp 84 and Trp 279 – present at the CAS and PAS, respectively. Peptides containing these two oxidized Trp residues were not detected when the competitive inhibitors, edrophonium and propidium (which should displace MB from the gorge) were present during illumination, in agreement with their efficient protection against the MB-induced photo-inactivation. Thus, the bound MB elicited selective action of $^1O_2$ on Trp residues facing onto the water-filled active-site gorge. Our findings thus demonstrate the localized action and high specificity of MB-sensitized photo-oxidation of *Tc*AChE, as well as the value of this enzyme as a model system for studying the mechanism of action and specificity of photosensitizing agents.

[¶]Corresponding author: Dr. Mathilde M. Triquigneaux, Laboratory of Toxicology and Pharmacology, NIH/National Institute of Environmental Health Sciences, 111 T.W. Alexander Drive, Research Triangle Park, NC 27709, USA, Phone: +1 (919) 541-3381, triquigneauxm@mail.nih.gov.

Keywords

Acetylcholinesterase; active site gorge; singlet oxygen; site-specific photo-oxidation; *N*-formylkynurenine; anti-NFK antiserum; mass spectrometry

INTRODUCTION

The principle biological role of acetylcholinesterase (AChE) is the termination of impulse transmission at cholinergic synapses by rapid hydrolysis of the neurotransmitter acetylcholine (ACh) [1]. In keeping with its biological role, AChE possesses very high specific activity, functioning at a rate approaching that of a diffusion-limited reaction [2]. The toxicity of organophosphate nerve agents and insecticides is due to their potent inhibition of AChE [3]. The first generation of drugs for the treatment of Alzheimer's disease are AChE inhibitors that act to overcome the cholinergic insufficiency resulting from degeneration of cholinergic nerve endings [4,5].

The electric organs of *Torpedo californica* and *Electrophorus electricus* are rich sources of AChE that is structurally homologous to that found in mammalian nerve and muscle [6]. Unexpectedly for such a rapid enzyme, the crystal structure of *Torpedo californica* AChE (*Tc*AChE) revealed that its active site is near the bottom of a deep and narrow gorge lined by the rings of 14 conserved aromatic residues [7]. It contains two subsites: a catalytic triad very similar to that found in other serine hydrolases, and a so-called catalytic 'anionic' site (CAS), which recognizes the quaternary group of ACh. A peripheral 'anionic' site (PAS) at the entrance to the active site gorge mediates substrate trapping [8]. At both sites, recognition of ACh is primarily via π-cation interactions with conserved aromatic residues [9,10].

Recently, Weiner et al. [11] investigated the interaction of methylene blue (MB) with *Tc*AChE. Methylene blue is a singlet-oxygen ($^1O_2$)-generating photosensitizer that is also a strong reversible inhibitor of *Tc*AChE in the dark [12,13]. The mechanism of generation of $^1O_2$ by light irradiation of MB is shown in Fig. 1a. The principal amino acid residues in proteins oxidized by $^1O_2$ are His, Cys, Met, Tyr and Trp. Oxidation of Trp residues results in the formation principally of *N*-formylkynurenine (NFK) and kynurenine (Fig. 1b). The MB/*Tc*AChE complex was used as a model system for studying the chemical and structural consequences of photo-oxidation of residues within the active-site gorge (it is assumed, *a priori*, that the photochemical properties of MB in its complex with *Tc*AChE, *viz.*, the life time of MB* and the efficacy of energy transfer to oxygen are similar to its properties in its uncomplexed state).

Indeed, illumination of *Tc*AChE in the presence of MB produces time- and concentration-dependent inactivation of the enzyme, attributable to $^1O_2$. Addition of reversible inhibitors of *Tc*AChE, such as edrophonium (ED), which interacts at the CAS [10], prior to sample illumination in the presence of MB protects the enzyme from inactivation, suggesting that the $^1O_2$ produced by MB is localized to the active-site gorge.

As mentioned, *Tc*AChE contains 14 highly conserved aromatic amino acid residues that line ~40% of its surface [7]. Both the CAS and the PAS contain a tryptophan residue, Trp 84 and Trp 279, respectively (*Tc*AChE numbering) [10]. The crystal structure of the MB/*Tc*AChE complex [14,15] (Protein Data Bank entry 2w9i) reveals a single MB molecule stacked against Trp 279, at the top or the gorge, and oriented along the gorge axis towards the active site (Fig. 2). Comparison of the fluorescence spectra of photo-inactivated *Tc*AChE and of

the native protein showed changes characteristic of Trp modification that are also correlated with loss of activity [11].

This study was undertaken to characterize and identify the specific structural modifications produced in the Trp residues of *Tc*AChE by MB photo-inactivation. We used a recently developed antiserum to *N*-formyl-kynurenine [16,17], an oxidation product of Trp and of Trp residues (Fig. 2), in Western analysis of *Tc*AChE samples that had been photo-oxidized in the presence of MB. A correlation was revealed between photo-inactivation of *Tc*AChE and Trp oxidation to NFK. Mass spectrometry was then used to precisely identify which of the 14 Trps of *Tc*AChE were oxidized to NFK in the photo-inactivated samples, as well as to identify other potential structural Trp modifications. It was revealed that MB-mediated photo-oxidation involves primarily Trp 84, within the CAS, and Trp 279, within the PAS.

EXPERIMENTAL

Materials

Guanidine hydrochloride, DL-dithiothreitol (>99%), iodoacetamide (bioUltra, >99%) and PNGase F (from *Elizabethkingia miricola*, solution in 20 mM Tris HCl, pH 7.5, 50 mM NaCl and 1 mM EDTA) were obtained from Sigma (St. Louis, MO). Trypsin and chymotrypsin (from bovine pancreas, modified, sequencing grade) were obtained from Roche Molecular Biochemicals (Indianapolis, IN). The anti-NFK serum was collected from immunized New Zealand White rabbits (Harlan Bioproducts, Madison, WI, USA). All other chemicals were of analytical grade and were purchased from Sigma or Roche Molecular Biochemicals.

Photo-oxidation

Purification and photo-oxidation of *Tc*AChE samples were performed as previously described [11].

Protein Gel Electrophoresis and Western Analyis

Ten μg aliquots of each sample were electrophoresed with SDS under reducing conditions (50 mM DTT) through duplicate 4–12% BisTris gels (Invitrogen). One gel was stained with Coomassie blue, and the second gel was transferred to nitrocellulose for Western analysis using rabbit polyclonal antiserum to NFK at a 1:1000 dilution, essentially as previously described [16]. Detection of NFK-containing proteins was performed using an Odyssey imager (Licor).

Protein Digestion

Lyophilized samples were solubilized in 100 mM phosphate buffer, pH 7.4, to a final concentration of 2 μM in *Tc*AChE, and 5 μL aliquots were treated in a dark room for mass spectrometry analysis. Samples were mixed with 5M guanidine-HCl for 30 minutes at 50°C and treated with 4.8 mM DTT for 30 minutes at 25°C, then 14.1 mM iodoacetamide was added and the sample incubated for 30 minutes at 25°C. Samples were diluted to 0.1 pmol/μL with 100 mM Tris-HCl, pH 8.5, just prior to deglycosylation with PNGase overnight at 37°C, and finally digested with chymotrypsin or trypsin at a protein:enzyme ratio of 20:1 at pH 8.0 for 8h at 37°C.

Mass Spectrometry

A Waters Q-TOF Premier mass spectrometer equipped with a nanoAcquity UPLC system and NanoLockspray source was used for the acquisition of the LC-ESI/MS^e [18,19] and LC-ESI/MS/MS data. Separations were performed using a 3 μm nanoAcquity Atlantis dC18

(100 μm × 100 mm) column (Waters) at a flow rate of 300 nL/min. A 5 μm nanoAcquity Symmetry C18 (100 μm × 20 mm) trapping column (Waters) was positioned in-line with the analytical column. Injections of 10 pmol of *Tc*AChE digests were made onto the column. Peptides were eluted using a linear gradient from 98% solvent A [water/0.1% formic acid (v/v)] and 2% solvent B [acetonitrile/0.1% formic acid (v/v)] to 95% solvent B over 120 min. Mass spectrometer settings for MS analyses were a capillary voltage of 3.5 kV, a cone voltage of 30 V, a source temperature of 80°C, and a collision energy of 4 eV. The mass spectra were recorded over a scan range of 100−2000 Da. MS data were acquired using a MS^e scanning approach in which two sets of MS data were collected: 1) low-energy LC/MS data, comprising MS data for peptide precursors with a collision energy of 4 eV, and 2) elevated energy MS data (15–35 eV ramp), which contains fragment ions. Ions of peptides identified in MS^e were then targeted for MS/MS acquisition with a collision energy of 15–45 eV ramp. All MS/MS spectra were manually validated. For calibration, an external lock mass was used with a separate reference spray (LockSpray) using a solution of glu-fibrinopeptide B (300 fmol/μL) in water/acetonitrile 80:20 (v/v) with 0.1% formic acid and a mass of 785.8496 (2+). Semi-quantitative analyses of *N*-formylkynurenine derivates were performed in triplicate, acquired in the MS-only mode, with injections of 10 μL of sample onto the column. LC/MS, LC-ESI/MS^e and LC-ESI/MS/MS data analyses were performed using MassLynx version 4.0 (Waters) and ProteinLynx softwares supplied by the manufacturer.

RESULTS

Immunological detection of NFK in methylene blue photooxidized *Tc*AChE

*Tc*AChE mixed with MB, or MB plus the protein inhibitors edrophonium and propidium (ED + PR), was irradiated for 1, 5, 10, or 20 min as previously described [11]. Additionally, samples consisting of *Tc*AChE alone, *Tc*AChE with MB, and *Tc*AChE with MB + ED + PR were maintained in the dark. Samples were then subjected to SDS-PAGE electrophoresis for parallel examination by Coomassie blue staining and anti-NFK western blotting (Fig. 3). The stained gel confirms that all lanes contained equal amounts of protein. This gel also shows that the lanes with the MB-containing protein subjected to the longest duration of illumination (Fig. 3, lane 6), as well as all of the light-exposed samples containing MB and the two AChE inhibitors (Fig. 3, lane 8–11), contain distinct bands of approximately 38 and 28 kD. However, the staining of these additional bands appears minor compared to the signal of *Tc*AChE protein at 65 kDa, and the anti-NFK western blot indicates that these fragments do not contain NFK residue. The anti-NFK western blot shows that while the MB-containing protein subjected to the longest duration of illumination stained strongly for NFK (Fig. 3, lane 6), the comparable sample containing the AChE inhibitors stained only very weakly at 65 kDa (Fig. 3, lane 11).

Mass spectrometry identification of tryptophan residue oxidation products

Although Figure 3 shows that NFK accumulates in photo-oxidized *Tc*AChE, western data cannot define which specific tryptophan residue(s) has been modified to NFK. Mass spectrometry was therefore used to identify which of the 14 tryptophan residues in *Tc*AChE were oxidized to kynurenine (Trp + 4 Da), hydroxy-tryptophan (Trp + 16 Da) and *N*-formylkynurenine (Trp + 32 Da) [20,21].

MS^e scanning was used, in which each ion detected for a specific retention time was fragmented without the selection of a precursor ion [18,19]. This allowed the collection of two sets of MS data, the first consisting of low-energy LC-MS data, comprising MS data for peptide precursors, and the second as elevated energy LC-MS^e data containing fragment ions. These two sets of MS^e data were then combined into “pseudo MS/MS” spectra for

each precursor ion. Because MS^e scanning imparts a high sensitivity, almost complete sequence coverage was obtained for both chymotrypsin and trypsin digests of the protein. Specifically, thirteen of the 14 tryptophan residues were detected, all but Trp 58. More importantly, LC-MS^e results provided information concerning the two tryptophan residues, Trp 84 and Trp 279, localized in the active- site gorge and suspected to be the main targets of the singlet oxygen reaction [11].

While thirteen of the fourteen tryptophan-containing peptides were detected by LC/MS^e analysis, only four contained oxidative modifications of +16, +32, +48 and/or +64 Da after 60 min of irradiation in the presence of MB (Table 1). Comparable analysis of a control *Tc*AChE sample did not detect the modifications found in peptides containing Trp 84, Trp 279 or Trps 432/435, indicating that the alterations in these peptides were due to irradiation in the presence of MB. However, in the case of Trp 233, an equivalent peptide with the addition of 32 Da was detected in control samples and could be attributed to an artifact generated during sample preparation. As summarized in Table 1, LC/MS^e results showed the oxidation of tryptophan-containing peptides due to MB-mediated photo-oxidation of *Tc*AChE. Nevertheless, despite the detection of these oxidized derivatives, fragmentation of the precursor ions in MS^e was insufficiently informative to clearly identify tryptophan as the primary oxidized residue of the modified peptides. Indeed, MS^e data are a complex mixture of fragment ions that do not allow the assignment of daughter ions to a specific precursor. Moreover, it appears that several *Tc*AChE methionine residues were easily oxidized during sample preparation for mass spectrometry analysis because identically modified peptides were detected in control samples containing *Tc*AChE. Because these data did not provide a clear distinction between oxidation on methionine residues and oxidation on tryptophan residues, LC-MS/MS experiments were performed targeting oxidized peptides detected in the MS^e mode to disambiguate the localization of NFK derivatives in *Tc*AChE.

Analysis of peptide containing Trp 279—Figure 4 presents the MS/MS spectrum of the ion *m/z* 826.4^{3+}, which could be assigned to the protonated peptide 270–289 with an additional 32 Da. Upon collision-induced dissociation (CID), this precursor ion showed a fragmentation pattern similar to that of the corresponding unmodified peptide, and gave rise mainly to amino-terminal b ions and acid-terminal y ions [22,23]. The series b_{10}-b_{13} corresponded to a shift in mass of an additional 32 Da, while the series b_5-b_9 remained identical when compared to the same series in the MS/MS spectrum of the unmodified peptide. These data allowed the assignment of a NFK residue localized on position 279 of *Tc*AChE. This result was corroborated by MS/MS experiments targeting the precursor ion of the protonated peptide 268–289 with an additional 32 Da, detected at *m/z* 912.0^{3+}which also showed the formation of an identical oxidized product localized on Trp 279 (data not shown). Therefore, taken together, these results lead to the conclusion that Trp 279 is oxidized into NFK in the presence of singlet oxygen.

Analysis of peptide containing Trp 84—Ions corresponding in mass to protonated peptides 72–96, a segment that contains Trp 84, were observed at *m/z* 1047.3^{3+}, 1052.6^{3+}, 1058.0^{3+} and 1063.4^{3+} (Table 1). These would correspond to the addition of 16, 32, 48 or 64 Da, respectively, compared to the unmodified peptide. MS/MS spectra of precursor ions *m/z* 1047.3^{3+} and 1052.6^{3+} indicated oxidation of one or two methionine residues, Met 83 and/or Met 90, into sulfoxide (data not shown). As mentioned above, it appears that methionine residues were easily oxidized during MS sample preparation because similar artifacts were detected in control samples containing only *Tc*AChE.

However, the CID of ions *m/z* 1058.0^{3+} and 1063.4^{3+} suggests a +32 Da oxidation localized on residue 84. As shown in Figure 5, the fragmentation pattern of the precursor ion *m/z* 1063.4^{3+} showed the oxidation of Met 90 into sulfoxide. Indeed, the series b_{20}-b_{25} was

detected with a shift in mass of 64 Da, while the daughter ion b_{18} was detected with an additional 48 Da when compared to the same series in the MS/MS spectrum of an unmodified peptide. MS/MS data suggested that this additional 48 Da was localized on Met 83-Trp 84 residues because the fragmentation pattern showed a non-modified series b_4-b_9. Moreover, supplementary internal fragments which contain the Met 83-Trp 84 sequence, such as protonated 82–85, 77–86 and 74–84 fragments, were also detected with an additional 48 Da compared to unmodified fragments. Therefore, even if MS/MS spectrum of the precursor ion *m/z* 1063.4^{3+} did not allow differentiation between Met 83 and Trp 84 modifications, these data strongly suggest the oxidation of both Met 83 and Met 90 into sulfoxide and the formation of an NFK derivative of tryptophan localized on position 84.

These results were further supported by MS/MS experiments targeting the precursor ion, detected at *m/z* 1058.1^{3+}, containing an additional 48 Da, which showed a similar fragmentation pattern (data not shown). More particularly, MS/MS data clearly indicated that Met 90 was not oxidized, while daughter ions containing Met 83-Trp 84 residues showed a shift of 48 Da in mass when compared to the same series in the MS/MS spectrum of the unmodified peptide. Therefore, these results lead to the conclusion that Trp 84 is oxidized into NFK in the presence of singlet oxygen.

Analysis of peptide containing Trp 432 and Trp 435—Figure S1 shows the MS/MS spectrum of the precursor ion *m/z* 870.1^{3+}, which could be assigned to the protonated peptide 422–442 with an additional 48 Da. Upon CID, this precursor ion gave rise to mainly amino-terminal b ions and acid-terminal y ions. Although the signal-to-noise ratio of this MS/MS spectrum was relatively low, the detailed fragmentation derived from series b_8-b_{13} and y_{10}-y_{11} clearly showed that only daughter ions which contained Trp 432 were detected with a shift in mass of 32 Da, while Met 436 could be also oxidized into sulfoxide with an additional 16 Da. Supplementary internal fragments which contained Trp 432, such as protonated 425–433 and 431–434 fragments, were also detected with an additional 32 Da compared to unmodified fragments. It should be noted that fragmentation of the precursor ion *m/z* 870.1^{3+} indicated that Trp 435 was not oxidized. Therefore, these results led to the conclusion that Trp 432, but not Trp 435, was oxidized to NFK by MB-mediated photo-oxidation.

Analysis of peptide containing Trp 233—As mentioned above, trypsin digest of *Tc*AChE detected the formation of a Trp 233-containing peptide with an additional 32 Da, observed in MS spectra at *m/z* 1109.6^{3+} (Table 1). However, this ion was also detected in control samples containing only the enzyme, and thus was not a result of MB photo-oxidation. Nevertheless, Trp 233-containing peptides were also studied to identify artifacts induced by sample preparation for mass spectrometry. The MS/MS spectrum of the ion *m/z* 1109.6^{2+} can be assigned to the protonated peptide 222–242 with an additional 32 Da (Figure S2). Upon CID, the series y_{11}-y_{17} corresponded to a shift in mass of an additional 32 Da, while the series y_2-y_9 remained identical when compared to the same series in the MS/MS spectrum of the unmodified peptide. These data allowed the assignment of an NFK residue of Trp 233 of *Tc*AChE, probably generated during sample preparation for mass spectrometry.

Semi-quantification of NFK in samples with increasing photo-sensitization—It has previously been reported that *Tc*AChE irradiated in the presence of MB undergoes time- and concentration-dependent inactivation [11]. Therefore, additional experiments were performed to evaluate the relative amount of NFK residues *vs* unmodified tryptophan residues in relation to irradiation time of a *Tc*AChE/MB mixture. Because chymotrypsin primarily hydrolyses the peptide bonds of Tyr, Phe and Trp residues, meaning that structural modifications of Trp residues interfere with the enzyme activity, trypsin digests were used

for mass spectrometry semi-quantification of Trp modifications. Experiments were performed in triplicate and acquired in the MS mode only. Briefly, chromatograms were extracted for each Trp-containing peptide ion previously identified, and LC peaks of corresponding *m/z* were integrated. It should be noted that all charge states of peptides detected in MS spectra were considered to obtain the total area of unmodified peptides (A_U), peptides which contain methionine oxidized into sulfoxide (A_S), and NFK-containing peptides (A_{NFK}). The percentage of NFK derivates (R_{NFK}) was then calculated using the following equation: $R_{NFK} = A_{NFK} / (A_U + A_S + A_{NFK})$. The relative quantification of NFK derivatives was performed using *Tc*AChE/MB samples irradiated for 20 and 30 minutes.

As previously mentioned, modified peptides containing Trp 84 and Trp 279 were not detected in control samples containing only *Tc*AChE, indicating that NFK residues were generated only upon MB-mediated photo-oxidation. More precisely, the oxidation rate of these two tryptophan residues increased with irradiation time. As shown in Table 2, 10% and 7.6% of Trp 84 and Trp 279, respectively, were converted into NFK after 30 minutes of irradiation in the presence of MB. Despite the low rate of tryptophan oxidation, these results correlate with a loss of *Tc*AChE activity, which decreases to only 16% of native *Tc*AChE after 30 minutes of photo-oxidation.

It should be noted that MS analysis showed that the percentage of the NFK derivatives of Trp 233-containing peptide was constant and low (< 0.5%). As previously mentioned, the oxidation of Trp 233 was assumed to be an artifact generated during MS sample preparation because the oxidized derivative could be detected in the control sample containing only *Tc*AChE. Consequently, Trp 233 derivative artifacts generated for preparation of MS samples could be considered as negligible.

In contrast to Trp 84-, Trp 279- and Trp 233-containing peptides, quantification data for the Trp 432 NFK derivative were unreliable. Because protonated Trp 432-containing peptides were detected with only a low intensity in MS spectra, sizable errors would be introduced during integration of chromatographic peaks. Nevertheless, modified Trp 432-containing peptides were not detected in control samples containing only the enzyme, and analysis of samples irradiated for 60 min in the presence of MB clearly shows conversion of Trp 432 into NFK.

Effect of competitive inhibitors on the formation of N-formylkynurenine—

Previous work showed that reversible competitive inhibitors of *Tc*AChE protect the enzyme from photo-inactivation [11]. Indeed, gorge-spanning ligands such as ED provided substantial protection against $^1O_2$-mediated enzyme inactivation by binding within the active gorge of the protein. Therefore, additional MS experiments were performed to measure the protective effect of the competitive inhibitors ED and propidium (PR) on the oxidation of tryptophan residues to NFK.

In contrast to the *Tc*AChE/MB sample, the addition of the reversible inhibitors strongly prevented the formation of NFK. Indeed, compared to the signal observed with the *Tc*AChE/MB system, only a very small NFK signal was detected in the Trp 279-containing peptide when inhibitors were present during MB photo-oxidation (Figure 6a). Comparable analysis of the Trp 84-containing peptide found no NFK when ED and PR were added to the reaction mixture (Figure 6b). These results correlate well with protein activity measurements performed after 20 minutes of MB-mediated photo-oxidation. In the presence of ED and PR, *Tc*AChE enzyme activity was reduced to 63% of control while the parallel sample without these inhibitors had enzyme activity that was only 30% of control. This indicates that ED and PR prevent MB access to Trp 84 and Trp 279, efficiently protecting the enzyme from photo-inactivation caused by singlet oxygen.

DISCUSSION

A previous study [11] showed that MB, a strong reversible inhibitor of *Tc*AChE in the dark, binds within the active-site gorge and that subsequent illumination of this mixture produces $^1O_2$, which inactivates the enzyme via alteration of specific amino acid residues within the active gorge. This work also showed that *Tc*AChE inhibitors, including ED, could protect *Tc*AChE from MB-mediated photo-inactivation. Fluorescence spectroscopy revealed that photo-inactivation was accompanied by a decrease in the apparent tryptophan fluorescence signal and an increase in the apparent NFK fluorescence signal. Taken together, these data suggest that MB-mediated $^1O_2$-generation in the *Tc*AChE active-site gorge leads to the alteration of two tryptophan residues, Trp 279 and Trp 84, located at the entrance to the gorge and at the bottom of the gorge adjacent to the catalytic trio, respectively.

This study was undertaken to precisely identify the $^1O_2$-altered tryptophan residues resulting from MB-mediated photo-oxidation and to characterize the specific tryptophan oxidation product. Initially, Western analysis (Fig. 3) using highly specific anti-NFK antiserum [16,17] confirmed the spectroscopic results [11], detecting NFK in MB-photo-oxidized protein that was absent in native protein and substantially reduced in *Tc*AChE irradiated in the presence of both MB and the inhibitors. Next, LC/MS^e was used to identify and analyze 13 of the 14 tryptophan-containing peptides of *Tc*AChE and to examine the oxidative modifications found in the photo-oxidized sample.

Possible modification of several residues, in addition to Trp and Met, was considered in processing the MS^e data, including His, Tyr, Cys and Pro. However, no oxidation products of any of these residues were detected. Only four of the tryptophan-containing peptides showed oxidative modifications. Trp 233 contained an identical modification (+32 Da) in both the photo-oxidized sample and the control native sample, and this alteration was therefore attributed to oxidation occurring during sample preparation. The other three peptides, those containing Trp 84, Trp 279 and Trps 432/435, were also subjected to LC-MS/MS experiments to determine the exact localization of oxidized derivatives on tryptophan residues. The deconvoluted MS/MS spectra derived from these experiments (Figs. 45S1, S2) clearly allow the assignment of NFK residues to Trp 84, Trp 279 and Trp 432. While the signal-to-noise ratio for the LC peak from the peptide containing Trp 432 was too low for any semi-quantitative analysis to be performed, LC/MS analyses from the peptides containing Trp 84 and Trp 279 were sufficiently sensitive to allow the correlation between increasing irradiation in the presence of MB, increasing accumulation of NFK and decreasing enzyme activity. Furthermore, when *Tc*AChE samples irradiated in the presence of MB were compared with those irradiated with MB in the presence of ED and PR, the latter showed little or no tryptophan oxidation, respectively, of Trp 279 and Trp 84.

The distance traveled by $^1O_2$ R, will depend on the diffusion coefficient, D, and on its lifetime, τ [24]:

$$R^2 = 6\,D\tau$$

The values found experimentally for diffusion of $^1O_2$ in cells, D ~2–4×10^2 cm^2/sec and τ~10 μsec [25], predict R~ 500 Å, much larger than the radius of gyration of the catalytic subunit of *Tc*AChE (~50 Å) or the length of its active-site gorge (15–20 Å) [7]. However, once generated in a cellular or protein environment, $^1O_2$ is unlikely to travel far due to the presence of natural quenchers; thus, its primary reactions should occur close to its site of generation. The distances between MB and the 14 Trp residues in *Tc*AChE are listed in Table 3. The MS data revealed apparent oxidation by $^1O_2$ of only 4 Trp residues, all conserved. Of these, Trp 233 was modified to an equal extent in the dark and under

illumination, and Trp 432 displayed only a very low level of modification. Only Trp 84 and Trp 279, both within the active-site gorge, were extensively modified to their NFK degradation products, and the data displayed in Fig. 6 clearly show that in the presence of competitive inhibitors that displace MB from the gorge, their modification is completely prevented. Trp 279 is obviously the closest residue, stacked against MB. Trp 84, which is in the 'anionic' subsite of the active site and interacts with the quaternary group of ACh, and Trp 233, which is on the surface of the acyl pocket, are at about the same distance, 13.8 and 13.1 Å, respectively. But while the indole ring of Trp 84 is fully exposed to the active-site gorge, in the case of Trp 233, examination of the crystal structure of *Tc*AChE reveals that whereas the phenyl moiety of the indole ring points towards the gorge, the 5-membered ring, the putative target of $^1O_2$, is not exposed [26]. Of the remaining residues, Trp 432 is the closest, and indeed the peptide containing it is modified, albeit marginally. Restriction of significant oxidative damage to Trp 84 and Trp 279 in *Tc*AChE is in keeping with the proposal of a facilitated diffusion pathway for $^1O_2$ along a water-filled channel in the fluorescent protein KillerRed [27]. Indeed, the aqueous channel seen in KillerRed is reminiscent of the active-site gorge of *Tc*AChE.

CONCLUSION

These results have confirmed the formation of NFK in photo-oxidized *Tc*AChE and identified the two major sites of oxidation to be on Trp 84 and Trp 279, both involved in the substrate binding in the active-site gorge of the enzyme. Despite evidence from previous work [11] that MB-mediated photo-inactivation produces only a modest perturbation of the *Tc*AChE native structure, oxidation of these two Trp residues within the active site gorge have a profound effect on enzyme activity. The specificity of the reaction can be explained by the localized action of the singlet oxygen inside the gorge mouth of the enzyme due to the specific binding of methylene blue. Therefore, the present work confirms that *Tc*AChE is a valuable model for understanding the molecular basis of local photooxidative damage with selective modifications of the protein [15]. The data obtained are pertinent to our understanding of the mode of action of photosensitizers in photodynamic therapy (PTD) [25] and the model using the *Tc*AChE-MB system would be particularly valuable in studies devoted to related areas. Although the technique is clinically applied to treat various diseases such as macular degeneration, pathologicalmyopia, esophagus, lung, and skin cancer [28], understanding of the cytotoxic action of PDT at the molecular level is important both for development of more selective photosensitizers and for enhancement of their therapeutic efficacy.

Supplementary Material

Refer to Web version on PubMed Central for supplementary material.

Acknowledgments

This research was supported by the Intramural Research Program of the NIH, National Institutes of Environmental Health Sciences, projects ES050139 and ES050171. We would like to acknowledge Mary J. Mason and Dr. Ann Motten for their editing of the manuscript. We thank Joel Sussman, Harry Greenblatt and Moshe Ben-David for valuable discussions and help with the graphics.

Abbreviations

***Tc*AChE**	*Torpedo californica* acetylcholinesterase
ACh	acetylcholine

CAS	catalytic ‘anionic’ site
PAS	peripheral ‘anionic’ site
MB	methylene blue
Trp	tryptophan
NFK	*N*-formylkynurenine
ED	edrophonium
PR	propidium
LC	liquid chromatography
MS	mass spectrometry
SDS-PAGE	sodium dodecylsulphate-polyacrylamide gel electrophoresis.

REFERENCES

1. Silman I, Sussman JL. Acetylcholinesterase: ‘Classical’ and ‘non-classical’ functions and pharmacology. Curr. Opin. Pharmacol. 2005; 5:293–302. [PubMed: 15907917]
2. Hasinoff BB. Kinetics of acetylthiocholine binding to electric eel acetylcholinesterase in glycerol/water solvents of increased viscosity. Evidence for a diffusion-controlled reaction. Biochim. Biophys. Acta. 1982; 704:52–58. [PubMed: 7093289]
3. Koelle, GB. Cholinesterases and anticholinesterase agents. Berlin: Springer-Verlag; 1963. Cytological distributions and physiological functions of cholinesterases; p. 187-298.
4. Azevedo Marques L, Giera M, Lingeman H, Niessen WMA. Analysis of acetylcholinesterase inhibitors: bioanalysis, degradation and metabolism. Biomed. Chromat. 2011; 25:278–299.
5. Reinhard S, Thomas A. The cholinergic system in aging and neuronal degeneration. Behavioural in brain research. 2011; 221:555–563.
6. Bon S, Vigny M, Massoulie J. Asymmetric and globular forms of acetylcholinesterase in mammals and birds. Proc. Natd. Acad. Sci. U.S.A. 1979; 76:2546–2550.
7. Sussman JL, Harel M, Frolow F, Oefner C, Goldman A, Toker L, Silman I. Atomic structure of acetylcholinesterase from *Torpedo californica*: A prototypic acetylcholine-binding protein. Science. 1991; 253:872–879. [PubMed: 1678899]
8. Dvir H, Silman I, Harel M, Rosenberry TL, Sussman JL. Acetylcholinesterase: from 3D structure to function. Chem.-bio inter. 2010; 187:10–22.
9. Colletier J-P, Fournier D, Greenblatt HM, Stojan J, Sussman JL, Zaccai G, Silman I, Weik M. Structural insights into substrate traffic and inhibition in acetylcholinesterase. EMBO J. 2006; 25:2746–2756. [PubMed: 16763558]
10. Harel M, Schalk I, Ehret-Sabatier L, Bouet F, Goeldner M, Hirth C, Axelsen P, Silman I, Sussman JL. Quaternary ligand binding to aromatic residues in the active-site gorge of acetylcholinesterase. Proc. Natl Acad. Sci. USA. 1993; 90:9031–9035. [PubMed: 8415649]
11. Weiner L, Roth E, Silman I. Targeted oxidation of *Torpedo californica* Acetylcholinesterase by singlet oxygen. Photochem. Photobiol. 2011; 87:308–316. [PubMed: 21155827]
12. Allen MT, Lynch M, Lagos A, Redmond RW, Kochevar IE. A wavelength dependent mechanism for rose bengal-sensitized photoinhibition of red cell acetylcholinesterase. Biochim. Biophys. Acta. 1991; 1075:42–49. [PubMed: 1892865]
13. Tomlinson GM, Cummings D, Hryshko L. Photoinactivation of acetylcholinesterase by erythrosin B and related compounds. Biochem. Cell Biol. 1986; 64:515–522. [PubMed: 3017385]
14. Paz, A. Structural and functional studies on the cytoplasmic domains of cholinesterase-like adhesion molecules. Rehovot, Israel: Feinberg Graduate School, Weizmann Institute of Science; 2009.

15. Paz A, Roth E, Ashani Y, Xu Y, Shnyrov VS, Sussman JL, Silman I, Weiner L. Structural and functional characterization of the interaction of the photosensitizing probe methylene blue with *Torpedo californica* acetylcholinesterase. Protein Sci. 2012 in the press.
16. Ehrenshaft M, deOliveira Silva S, Perdivara I, Bilski P, Sik HR, Chignell CF, Tomer KB, Mason R. Immunological detection of *N*-formylkynurenine in oxidized proteins. Free Rad. Biol. Med. 2009; 46:1260–1266. [PubMed: 19353782]
17. Ehrenshaft M, Zhao B, Andley UP, Mason RP, Roberts JE. Immunological detection of N-formylkynurenine in porphyrin-mediated photooxided lens α-crystallin. Photochem. Photobiol. 2011; 87:1321–1329. [PubMed: 21770952]
18. Chakraborty AB, Berger SJ, Gebler JC. Use of an integrated MS – multiplexed MS/MS data acquisition strategy for high-coverage peptide mapping studies. Rapid Comm. Mass Spectrom. 2007; 21:730–744.
19. Plumb RS, Johnson KA, Rainville P, Smith BW, Wilson ID, Castro-Perez JM, Nicholson JK. UPLC/MS^E: a new approach for generating molecular fragment information for biomarker structure elucidation. Rapid Comm. Mass Spectrom. 2006; 20:1989–1994.
20. Schey KL, Finley EL. Identification of peptide oxidation by tandem mass spectrometry. Acc. Chem. Res. 2000; 33:299–306. [PubMed: 10813874]
21. Todorovski T, Fedorova M, Hoffmann R. Mass spectrometric characterization of peptides containing different oxidized tryptophan residues. J. Mass Spectrom. 2011; 46:1030–1038. [PubMed: 22012669]
22. Biemann K. Sequencing of peptides by tandem mass spectrometry and high-energy collision-induced dissociation. Methods Enzymol. 1990; 193:455–479. [PubMed: 2074832]
23. Seidler J, Zinn N, Boehm ME, Lehmann WD. De novo sequencing of peptides by MS/MS. Proteomics. 2010; 10:634–649. [PubMed: 19953542]
24. Crank, J. The Mathematics of Diffusion. Oxford: Oxford University Press; 1975.
25. Ogilby PR. Singlet oxygen: there is indeed something new under the sun. Chem. Soc. Rev. 2010; 39:3181–3209. [PubMed: 20571680]
26. Harel M, Quinn DM, Nair HK, Silman I, Sussman JL. The X-ray structure of a transition state complex reveals the molecular origin of the catalytic power and substrate specificity of acetylcholinesterase. J. Am. Chem. Soc. 1996; 118:2340–2234.
27. Roy A, Carpentier P, Bourgeois D, Field M. Diffusion pathways of oxygen species in the phototoxic fluorescent protein KillerRed. Photochem. Photobiol. Sci. 2010; 9:1342–1350. [PubMed: 20820672]
28. Dolmans DEJGJ, Fukumura D, Jain RK. Photodynamic therapy for cancer. Nat. Rev. Cancer. 2003; 3:380–387. [PubMed: 12724736]

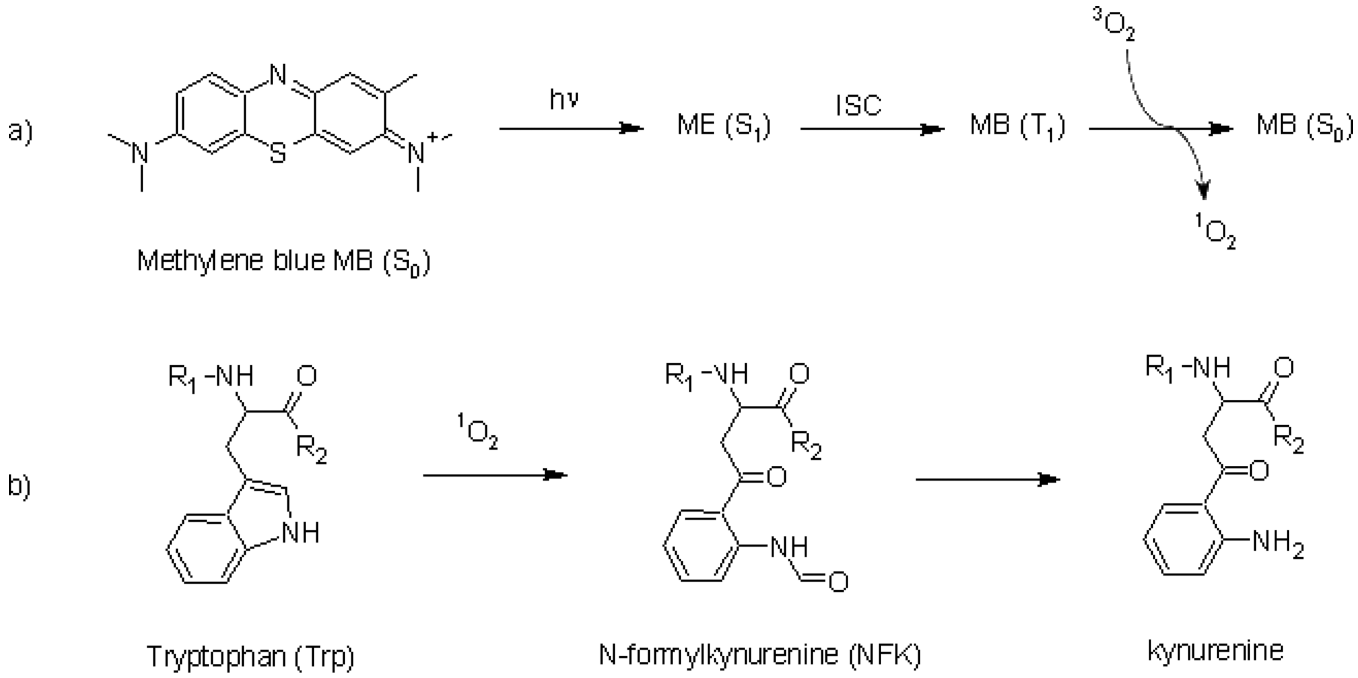

Figure 1.

Singlet oxygen formation from methylene blue and its reaction with Trp. a) Formation of singlet oxygen generated by the irradiation of methylene blue and b) oxidation of a tryptophan residue to NFK and kynurenine by $^1O_2$. (T_1: triplet state; ISC: intersystem crossing)

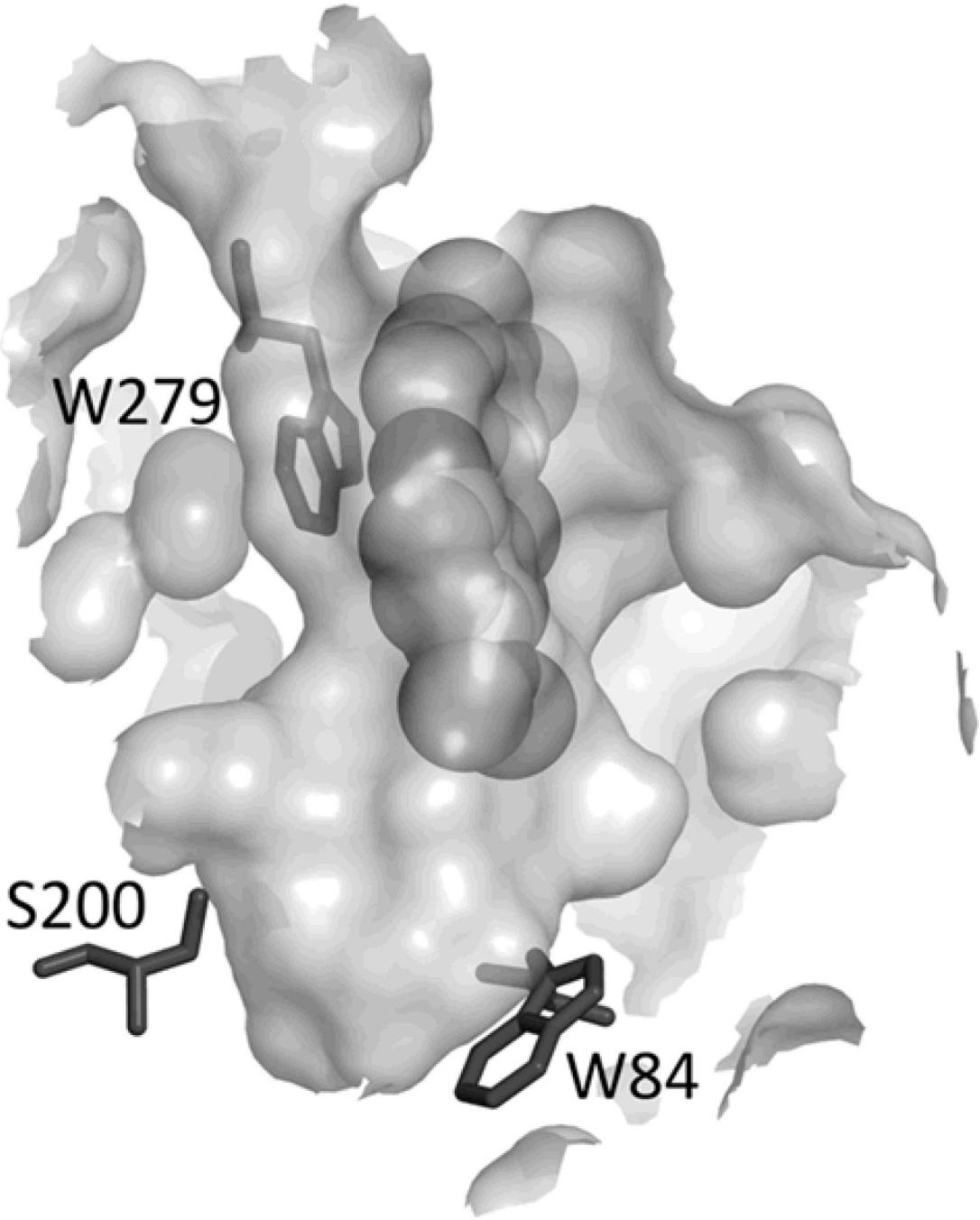

Figure 2.
Cross-section through the active-site gorge of *Tc*AChE in the MB/*Tc*AChE complex. The MB molecule is seen stacked against Trp 279 in the peripheral anionic site (PAS). Also shown are Trp 84, in the catalytic anionic subsite of the active site (CAS), and the active-site serine, Ser 200. The entrance to the gorge is depicted at the top. The crystal structure of the MB/*Tc*AChE complex has been deposited in the Protein Data Bank with access code 2W9I.

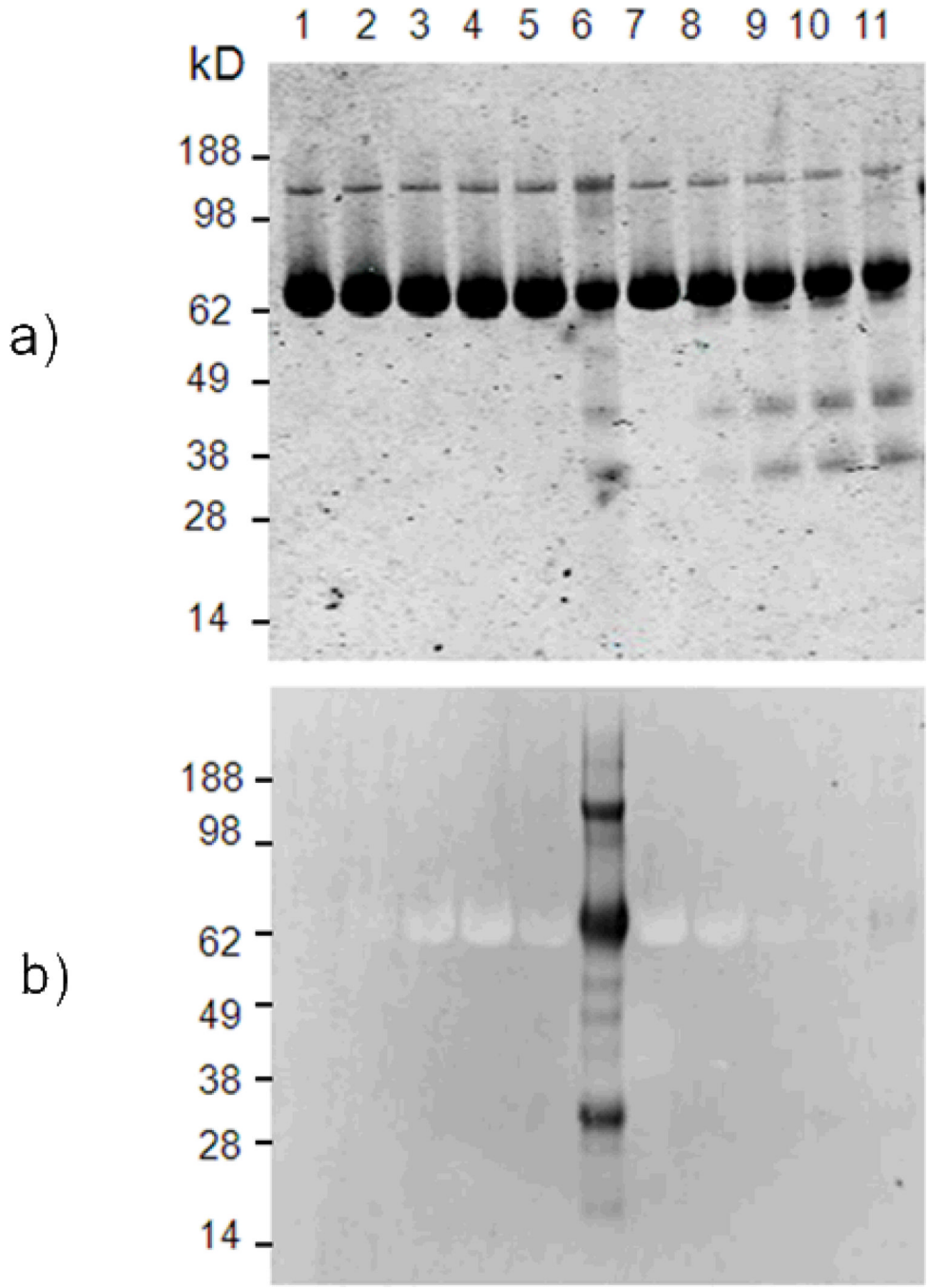

Figure 3.

Immunological detection of NFK in *Tc*AChE samples light-irradiated in the presence of MB. a) Coomassie blue staining and b) anti-NFK blotting of *Tc*AChE-containing samples. The protein (1) was mixed with MB (2) in the dark or further irradiated for (3) 1, (4) 5, (5) 10 or (6) 20 minutes. Other lanes correspond to the reaction of *Tc*AChE plus MB in the presence of inhibitors (7) in the dark or further irradiated for (8) 1, (9) 5, (10) 10 or (11) 20 minutes.

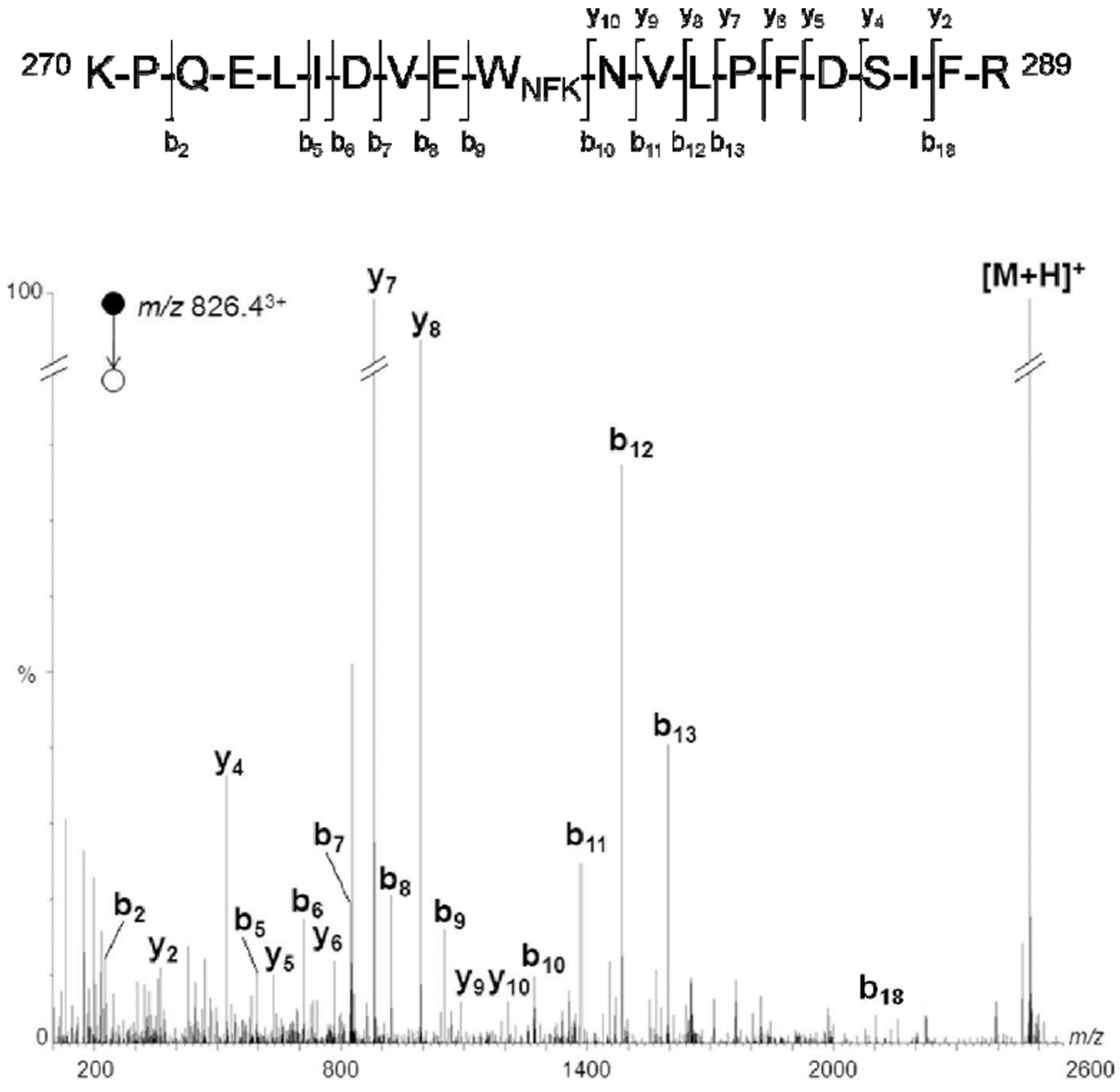

Figure 4.

Deconvoluted MS/MS spectrum acquired from a parent ion of *m/z* 826.4^{3+}, which corresponds in mass to tryptic peptide 270–289 + 32 Da. For the sake of clarity, not all identified fragment ions are labeled on the spectrum.

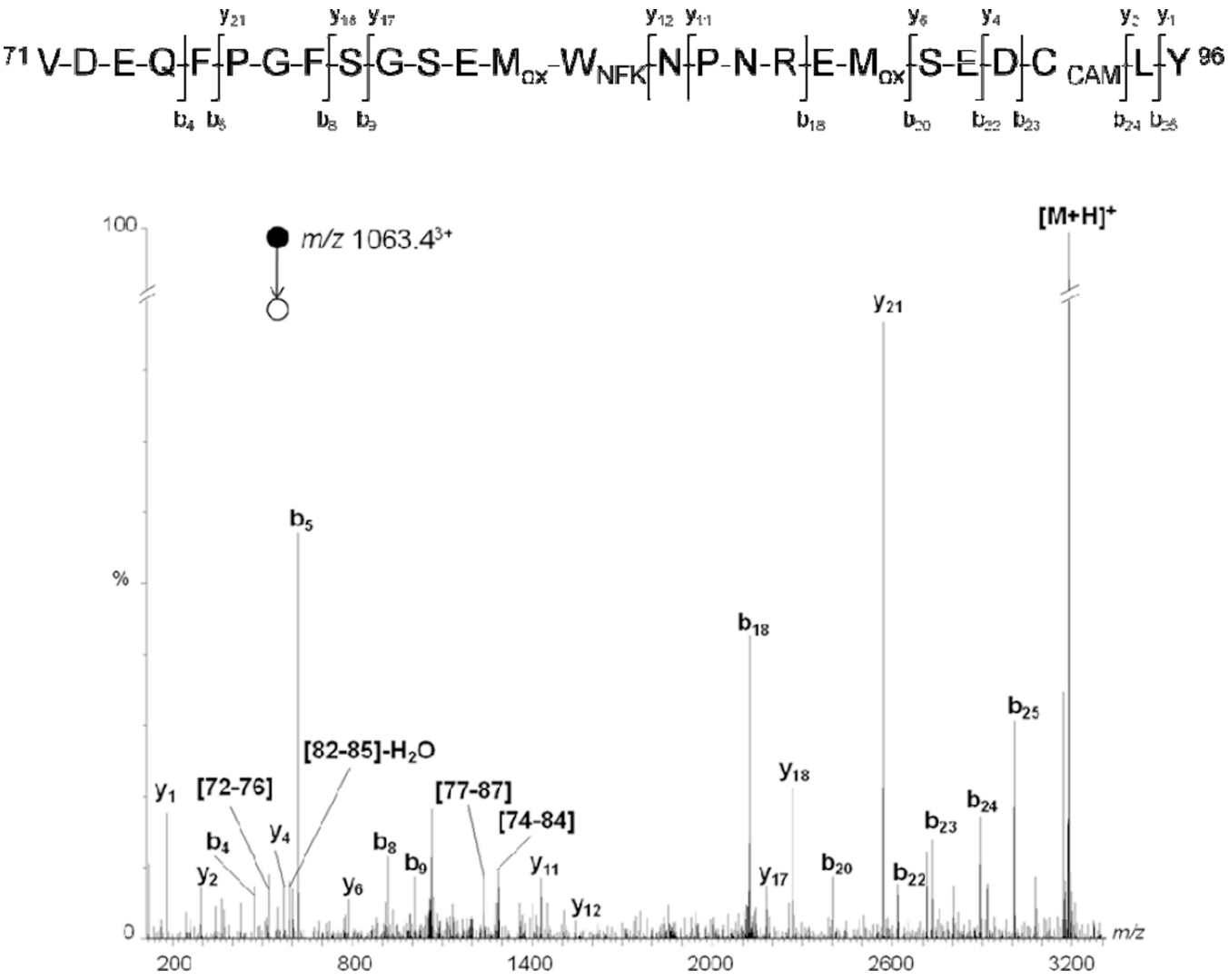

Figure 5.

Deconvoluted MS/MS spectrum acquired from a parent ion of *m/z* 1063.4^{3+}, which corresponds in mass to chymotryptic peptides 71–96 + 64 Da. For the sake of clarity, not all identified fragment ions are labeled on the spectrum.

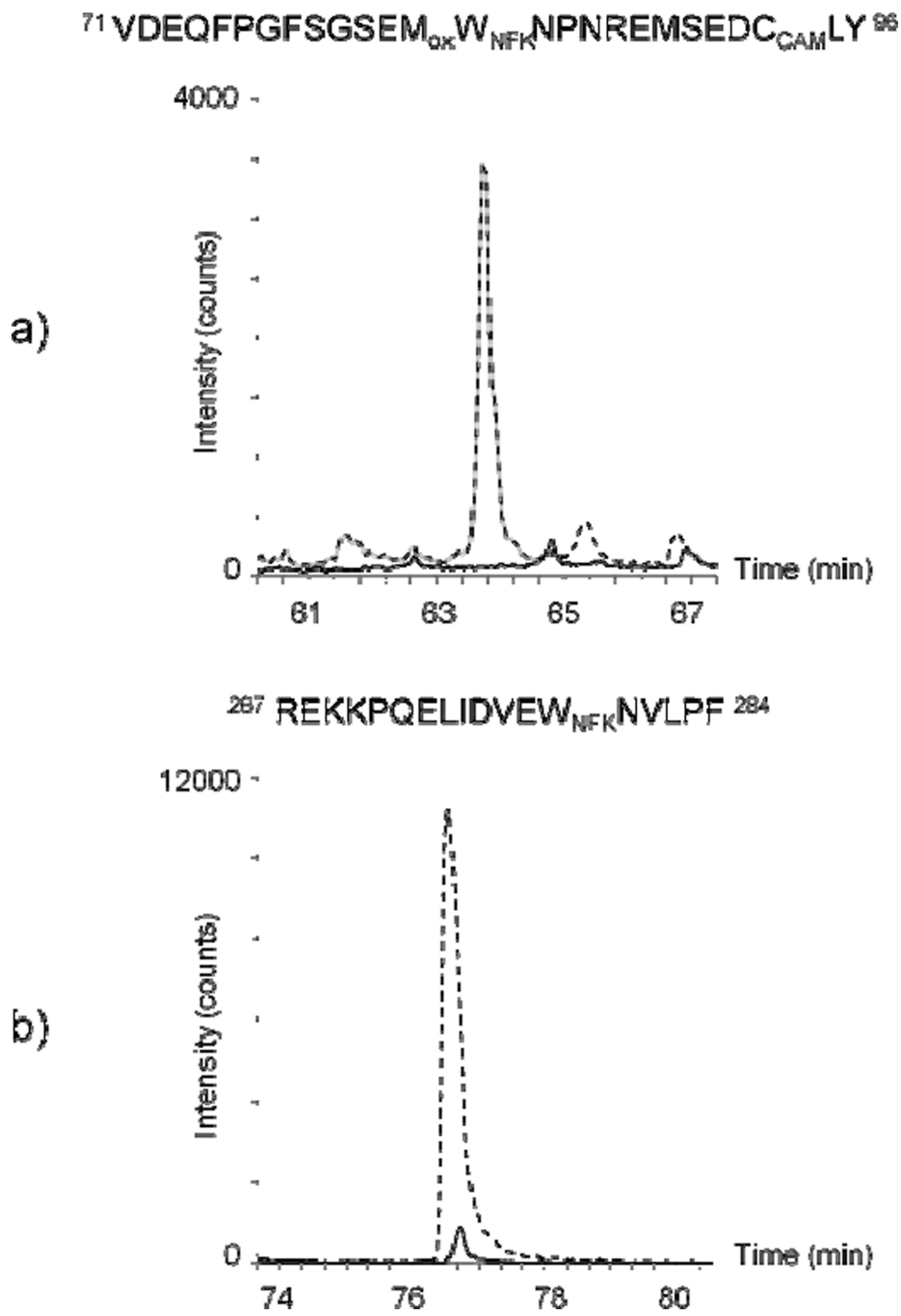

Figure 6.

Chromatograms of chymotryptic peptides which contain NFK derivatives from a) Trp 84 (*m/z* 1058.1^{3+}) and b) Trp 279 (*m/z* 632.3^{2+}), respectively. The signal intensity is indicated for the total ion current chromatogram. Analyses of samples containing *Tc*AChE plus MB further irradiated for 20 minutes are indicated by dotted lines (without the inhibitors, ED and PR) and solid lines (with the inhibitors).

Table 1

Trp-containing peptides with oxidative modifications[a,b] observed by LC/MS[c]. MS data were acquired using an MS[e] approach combining a low and an elevated-energy LC/MS set containing precursor ions and fragment ions, respectively.

Target	Peptide sequence	Modification	*m/z*
Trp 84	^{72}VDEQFPGFSGSEM**W**NPNREMSEDCLY^{96}	+16 Da +32 Da +48 Da +64 Da	1047.3^{3+} 1052.6^{3+} 1058.1^{3+} 1063.4^{3+}
Trp 233	^{222}AILQSGSPNCP**W**ASVSVAEGR^{242}	+32 Da	1109.6^{2+}
Trp 279	^{270}KPQELIDVE**W**NVLPFDSIFR^{289}	+32 Da	826.4^{3+}
	^{268}EKKPQELIDVE**W**NVLPFDSIFR^{289}	+32 Da	912.0^{3+}
Trp 432/435	^{431}V**W**PE**W**MGVIHGY^{442}	+16 Da	745.4^{2+}
	^{422}FFNHRASNLV**W**PE**W**MGVIHGY^{442}	+48 Da	870.1^{3+}
	^{424}NHRASNLV**W**PE**W**MGVIHGY^{442}	+16 Da	761.4^{3+}

[a] Modifications detected in MS correspond to the oxidation of several residues as follow: +16 Da = Met sulfoxide; +32 Da = NFK or two Met sulfoxides; +48 Da= Met sulfoxide plus NFK; +64 Da = two Met sulfoxides plus NFK.

[b] CAM indicates derivatization to carbamidomethyl derivatives of cysteine residues detected with an additional 57 Da.

[c] *Tc*AChE was identified using the Swiss Protein Data Bank (accession code P04058).

Table 2

Relative quantification of *N*-formylkynurenine derivates and *Tc*AChE activity

	Irradiation time (min)		
	0	**20**	**30**
Trp 84	N.D.	8.2%	10.0%
Trp 279	N.D.	3.7%	7.6%
Activity	100%	30%	16%

Table 3

Distances between Trp residues and MB in the MB/ *Tc*AChE complex[a]

Trp residue	Distance from MB (Å)
54	39.5
58	33.8
84	13.8
100	30.7
114	20.8
179	34.9
233	13.1
279	5.7
378	29.1
432	14.7
435	16.4
473	26.3
492	32.5
524	20.7

[a]The distances shown are from the aromatic nitrogen atom of MB to the aromatic nitrogens of the indole rings of the respective Trp moieties.